



LARGE SYNOPTIC SURVEY TELESCOPE

Large Synoptic Survey Telescope (LSST)

# Differential Chromatic Refraction: literature overview

I. S. Sullivan, and D. J. Reiss

DMTN-017

Latest Revision: 2015-12-02

## Contents

<b>1 Overview</b>	<b>1</b>
<b>2 DCR literature</b>	<b>1</b>
2.1 Report on Summer 2014 Production: Analysis of DCR [DMTN-070] . . . . .	1
2.2 Alcock et al. (1999) . . . . .	4
2.3 Hohenkerk & Sinclair (1985) . . . . .	5
2.4 Meyers & Burchat (2015) . . . . .	6
2.5 Chambers (2005) . . . . .	6
2.6 Alejandro Plazas & Bernstein (2012) . . . . .	6



2.7	Stone (1996)	7
2.8	Filippenko (1982)	9
2.9	Cuby et al. (1998)	9
2.10	Tomaney & Crotts (1996)	9
2.11	Mangum & Wallace (2015)	9
2.12	Auer & Standish (2000)	9

# Differential Chromatic Refraction: literature overview

## 1 Overview

Like any medium, the Earth's atmosphere refracts incident light, which for an observer on the Earth's surface results in a deflection of the apparent position of sources towards zenith by about 1 arcsecond per degree of the source from zenith. This bulk effect of refraction is well understood in astronomical applications and is easily accounted for most of the optical through radio wavelengths where the index of refraction is constant, but towards the blue end of the optical spectrum atmospheric dispersion results in increasing refraction. As a result, photons from the same source but different wavelengths that pass through the same filter of a telescope will have slightly different degrees of refraction and will land on different locations of the detector, an effect called Differential Chromatic Refraction (DCR). Differential Chromatic Refraction was first raised as an issue for spectrometry in Filippenko (1982), where the problem was framed as a loss of flux in slit spectrometers. The issue has now become important for imaging cameras as well, though, because high-resolution cameras such as the LSST will experience significant PSF smearing in the  $u$  and  $g$  bands (Figure 1).

## 2 DCR literature

A quick summary of and notes on the existing literature covering DCR. Each reference we found is covered in it's own subsection below.

### 2.1 Report on Summer 2014 Production: Analysis of DCR [DMTN-070]

- Estimated DCR effects directly for LSST using catSim's stellar SEDs.
- Investigated only airmass effects (no temperature, etc. dependence).
- Utilized 5 mas threshold for "good" DCR corrections based on estimated accuracy required for difference imaging (no dipoles).
- Summary of DCR estimates:
  - For  $g$  and  $r$ , nearly all stars will exhibit differential DCR of  $> 5$  mas at parallactic angle differences  $> 20$  deg. or airmass differences of  $> 0.15$ .

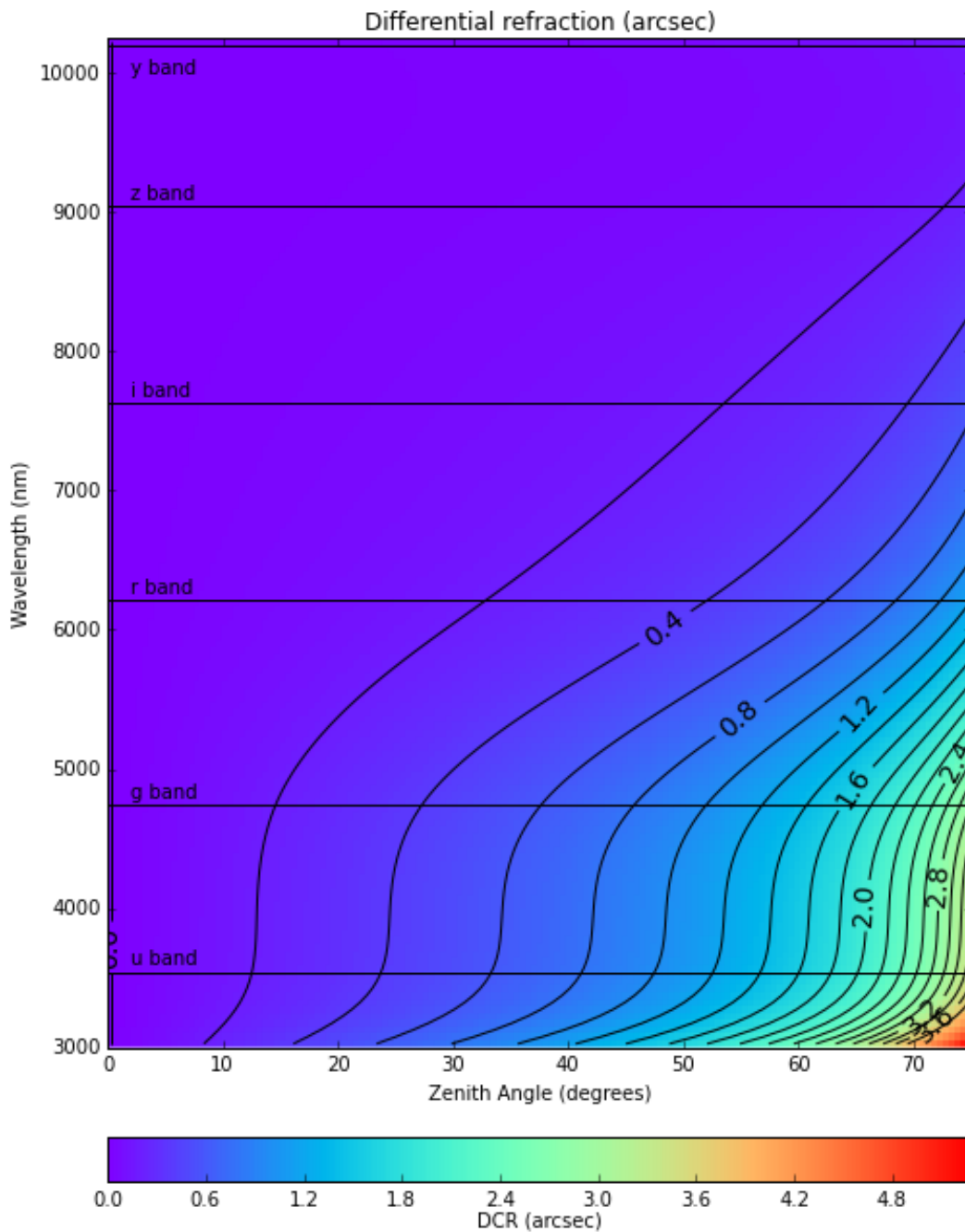


FIGURE 1: Maximum DCR over a range of zenith angles and wavelengths. Each wavelength is treated as the center wavelength of a band with bandwidth interpolated between the actual LSST bands (black lines), and maximum DCR is calculated for the difference in position of two photons from the same source at opposite ends of the band.

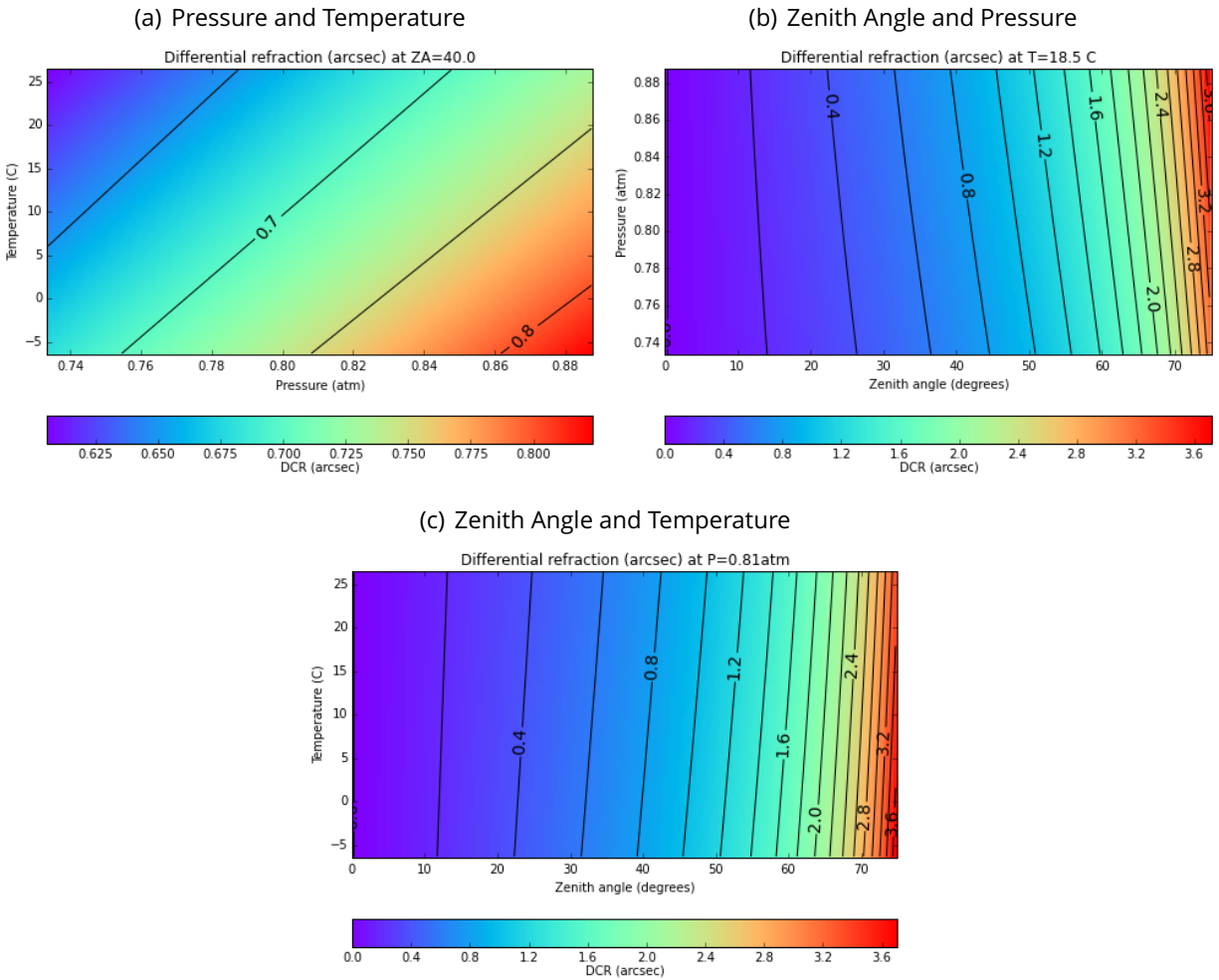


FIGURE 2: Investigation of maximum DCR under varying conditions for LSST  $u'$  band. For a given filter, maximum DCR depends on the zenith angle of observation (airmass), atmospheric pressure, temperature, and, to a lesser degree, humidity. In panels (a) - (c) we keep one of the three main parameters fixed at a nominal value, and map the full range of realistic observing conditions for the remaining two to get a feel for the relative importance of each.

- For  $i$ , similar effects for parallactic angle differences  $> 25$  deg. or airmass differences  $> 0.2$ , mostly for M-dwarf stars.
- For  $z$ , only very large differences in parallactic angle or airmass lead to DCR  $> 5$  mas.
- DCR corrections tested based on modeling using colors and airmass terms.
  - Random forest regression models provided most accurate modeling of DCR and refraction.
  - $u$  and  $g$  models worked but would be degraded by 10% color errors ( $u$ ) or 2.5% color errors ( $g$ ).
  - $riz$  models could correct all but  $10^{-5}$  stars to  $< 5$  mas residuals.

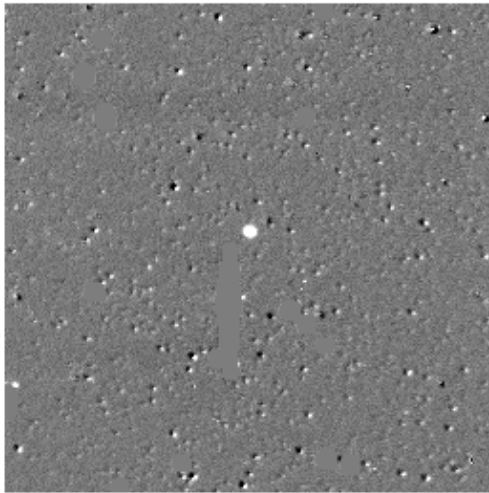
**\*\*Recommendations\*\*:**

- Code from the S14DCR analysis (<https://github.com/lstt-dm/DMTN-070>) should be updated to use latest version of `sims_photUtils` and include estimates for galaxies and SNe.
- Understand how DCR calcs are performed in `sims` pipeline to compare the results of these simulations to DCR effects in simulated images, and to enable investigation of DCR corrections on image coadds and differences (see also <https://github.com/lstt-dm/W14ImageDifferencing> and DMTN-069).

## 2.2 Alcock et al. (1999)

- Investigation of DiffIm for MaCHO search.
- This is the only reference I could find that described a method to correct for DCR for image differencing. Suggestion is to compute a per-pixel color map of each field (using images near zenith or at least at the same airmass and parallactic angle). They then interpolated the pixel values in the template image based on the color map pixel values, the airmass of the observation relative to the reference image, and the parallactic angle of the observation.

(a) Difference image with no DCR correction



(b) Difference image with DCR correction

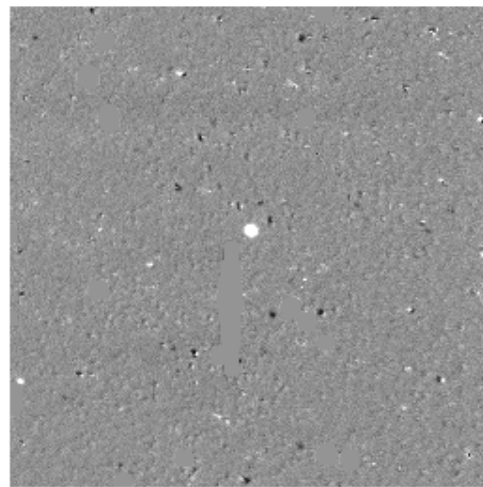


FIGURE 3: (Alcock et al. Fig. 5.)— "The effect of differential refraction on difference images. Left image is a difference image without applying any correction for differential refraction effects. The right image is the same image with our correction technique applied. The scale of the noise structures is much reduced although not completely removed. The two images are  $100'' \times 100''$ . The residual object in the centre is due to a variable star"

- Improvements were obtained by differencing a number of images taken at a range of airmasses to obtain a semi-empirical result for the offset required with color and air-mass (relative to the reference image).
- The results shown in Figure 3 suggest moderate success with this strategy.

### 2.3 Hohenkerk & Sinclair (1985)

- Good background.
- Uses a different implementation, "the method recommended by Auer and Standish".
- This is the function implemented in 'palpy' which is used by some (but not all?) code in the 'sims' stack.
- Uses a model atmosphere with temperature and pressure gradients, integrated to the surface. This I believe is different from Filippenko (1982) which assumes a single refractive surface.

## 2.4 Meyers & Burchat (2015)

- Estimates of DCR on weak lensing measurements.
- Source code for analysis is available here: <https://github.com/DarkEnergyScienceCollaboration/chroma/>.
- Primarily measured effects of DCR on shape measurements (2nd moments); code can be used to estimate 1st moments for a given SED. Preliminary code: <https://github.com/isullivan/LSST-DCR/tree/master/code/notebooks>.
- Also investigated effects of 1st moments for galaxy SEDs and compensation via extra trees regression on LSST colors.

## 2.5 Chambers (2005)

- Updated summary of (more accurate?) astrometric transformations including DCR.
- Estimated astrometric accuracy in Pan-STARRS of 1 mas. This assumes accurate atmospheric characterization for each field from sky probes (atmospheric absorption).

**\*\*Recommendations\*\*:**

- Understand these transformations. Suggestion is that C code exists somewhere in the Pan-STARRS codebase, but I could not find it.

## 2.6 Alejandro Plazas & Bernstein (2012)

- Investigates the effect of DCR on weak lensing measurements through the second moment of galaxy shape measurements.
- Finds that "Using standard galaxy and stellar spectral templates we calculate the resultant errors in the griz bands, and find that atmospheric dispersion shear systematics, left uncorrected, are up to 6 and 2 times larger in g and r bands, respectively, than the thresholds at which they become significant contributors to the DES error budget, but can be safely ignored in i and z bands. For the stricter *LSST* requirements, the factors are about 30, 10, and 3 in g, r, and i bands, respectively"



## 2.7 Stone (1996)

- A good reference giving equations for refraction including the effect of temperature, pressure, and water vapor pressure. Used for calculating Figure 2 We summarize the environmental and observing condition parameters in Table 1 and list the units and range of validity for the equations for each.

Parameter	valid range	description	units
$P_s$	$0 \text{ mbar} < P_s < 4000 \text{ mbar}$	Atmospheric pressure	millibar
$RH$	$0\% < RH < 100\%$	Relative humidity	Percent
$\lambda$	$2302\text{\AA} < \lambda < 20,586\text{\AA}$	Wavelength	Angstroms
$T$	$250\text{K} < T < 320\text{K}$	Temperature	Kelvin
$\phi$	$0^\circ \leq \phi < 360^\circ$	Latitude of the observing site	Degrees
$h$	$0 \text{ m} \leq h$	Elevation of the observing site	meters
$z_0$	$0^\circ \leq z_0 < 75^\circ$	Zenith angle	Degrees

TABLE 1: Definition of parameters and their units

The refraction of monochromatic light is given by

$$\begin{aligned}
 R(\lambda) &= r_0 n_0(\lambda) \sin z_0 \int_1^{n_0(\lambda)} \frac{dn}{n (r^2 n^2 - r_0^2 n_0(\lambda)^2 \sin^2 z_0)^{1/2}} \\
 &\simeq \kappa(n_0(\lambda) - 1)(1 - \beta) \tan z_0 - \kappa(1 - n_0(\lambda)) \left( \beta - \frac{n_0(\lambda) - 1}{2} \right) \tan^3 z_0
 \end{aligned} \tag{1}$$

where  $n_0(\lambda)$ ,  $\kappa$ , and  $\beta$  are given by equations 2, 3, and 4 below, respectively.

To calculate refraction, we need to know the local index of refraction of air  $n_0(\lambda)$  at the observatory site:

$$n_0(\lambda) = 1 + \left( \left[ 2371.34 + \frac{683939.7}{130 - \sigma(\lambda)} + \frac{4547.3}{38.9 - \sigma(\lambda)^2} \right] D_s + (6487.31 + 58.058\sigma(\lambda)^2 - 0.71150\sigma(\lambda)^4 + 0.08851\sigma(\lambda)^6) P_w \right) \quad (2)$$

where

$$\sigma(\lambda) = 10^4/\lambda \quad (\mu m^{-1})$$

$$D_s = \left[ 1 + (P_s - P_w) \left( 57.90 \times 10^{-8} - \frac{9.3250 \times 10^{-4}}{T} + \frac{0.25844}{T^2} \right) \right] \frac{(P_s - P_w)}{T}$$

$$D_w = \left[ 1 + P_w \left( 1 + 3.7 \times 10^{-4} P_w \right) \left( -2.37321 \times 10^{-3} + \frac{2.23366}{T} - \frac{710.792}{T^2} + \frac{7.75141 \times 10^4}{T^3} \right) \right] \frac{P_w}{T}$$

$$P_w = RH \times 10^{-4} \times e^{(77.3450 + 0.0057T - 7235.0/T)/T} T^{8.2}$$

where the parameters  $D_s$  and  $D_w$  are the density factors for dry air and water vapor, respectively, taken from Owens (1967).

The ratio of local gravity at the observing site to  $g = 9.81 m/s^2$  is given by

$$\kappa = g_0/g = 1 + 5.302 \times 10^{-3} \sin^2 \phi - 5.83 \times 10^{-6} \sin^2(2\phi) - 3.15 \times 10^{-7} h \quad (3)$$

If we assume an exponential density profile for the atmosphere, then the ratio  $\beta$  of the scale height of the atmosphere to radius of the observing site from the Earth's core can be approximated by:

$$\begin{aligned} \beta &= \frac{1}{R_\oplus} \int_0^\infty \frac{\rho}{\rho_0} dh \\ &\simeq \frac{P_s}{\rho_0 g_0 R_\oplus} = \frac{k_B T}{m g_0 R_\oplus} \\ &= 4.5908 \times 10^{-6} T \end{aligned} \quad (4)$$

where  $m$  is the average mass of molecules in the atmosphere,  $R_\oplus$  is the radius of the Earth,  $k_B$  is the Boltzmann constant, and  $g_0$  is the acceleration due to gravity at the Earth's surface.

## 2.8 Filippenko (1982)

- Original paper posing DCR as a problem to be addressed. Mostly of historical interest.
- Focused on the effect on spectrometers, with the recommendation that slit spectrometers be aligned with fixed parallactic angle.

## 2.9 Cuby et al. (1998)

- As with Filippenko, concerned with flux loss in slit spectrometers.
- Discusses observing strategies for spectrometers to keep flux loss  $< 20\%$  at  $z_0 < 50^\circ$

## 2.10 Tomaney & Crotts (1996)

## 2.11 Mangum & Wallace (2015)

## 2.12 Auer & Standish (2000)

## References

Alcock, C., Allsman, R.A., Alves, D., et al., 1999, ApJ, 521, 602 (arXiv:astro-ph/9903215), doi:10.1086/307567, ADS Link

Alejandro Plazas, A., Bernstein, G., 2012, PASP, 124, 1113 (arXiv:1204.1346), doi:10.1086/668294, ADS Link

Auer, L.H., Standish, E.M., 2000, AJ, 119, 2472, doi:10.1086/301325, ADS Link

**[DMTN-069]**, Becker, A.C., Krughoff, K.S., Connolly, A., 2014, *Report on Winter 2014 Production: Image Differencing*, DMTN-069, URL <https://dmtn-069.lsst.io>, LSST Data Management Technical Note

**[DMTN-070]**, Becker, A.C., Krughoff, K.S., Connolly, A., 2014, *Report on Summer 2014 Production: Analysis of DCR*, DMTN-070, URL <https://dmtn-070.lsst.io>, LSST Data Management Technical Note

- Chambers, K.C., 2005, In: Seidelmann, P.K., Monet, A.K.B. (eds.) *Astrometry in the Age of the Next Generation of Large Telescopes*, vol. 338 of *Astronomical Society of the Pacific Conference Series*, 134, [ADS Link](#)
- Cuby, J.G., Bottini, D., Picat, J.P., 1998, In: D'Odorico, S. (ed.) *Optical Astronomical Instrumentation*, vol. 3355 of *Proc. SPIE*, 36–47, doi:10.1117/12.316769, [ADS Link](#)
- Filippenko, A.V., 1982, *PASP*, 94, 715, doi:10.1086/131052, [ADS Link](#)
- Hohenkerk, C., Sinclair, A., 1985, *NAO Technical Note*, 63, URL <http://astro.ukho.gov.uk/data/tn/naotn63.pdf>
- Mangum, J.G., Wallace, P., 2015, *PASP*, 127, 74 (arXiv:1411.1617), doi:10.1086/679582, [ADS Link](#)
- Meyers, J.E., Burchat, P.R., 2015, *ApJ*, 807, 182 (arXiv:1409.6273), doi:10.1088/0004-637X/807/2/182, [ADS Link](#)
- Owens, J.C., 1967, *Appl. Opt.*, 6, 51, doi:10.1364/AO.6.000051, [ADS Link](#)
- Stone, R.C., 1996, *PASP*, 108, 1051, doi:10.1086/133831, [ADS Link](#)
- Tomaney, A.B., Crotts, A.P.S., 1996, *AJ*, 112, 2872 (arXiv:astro-ph/9610066), doi:10.1086/118228, [ADS Link](#)